

Supporting Information

I. Materials and Methods	2
II. UV-Vis Spectroscopic Investigation.....	3
III. NMR Spectroscopic Investigation.....	4
IV. Crystal Structure Solution and Refinement.....	7
V. Computational Details.....	12
VI. References.....	14

I. Materials and Methods

All manipulations were carried out using break-and-seal^[1] and glove-box techniques under an atmosphere of argon. Tetrahydrofuran (THF) and hexanes (Sigma Aldrich) were dried over Na/benzophenone and distilled prior to use. THF-*d*₈ (Sigma Aldrich) was dried over NaK₂ alloy and vacuum-transferred. TIPS-PPP (**1**) was prepared according to a procedure described earlier^[2] and heated in an evacuated ampule at 270 °C (to remove some oil) prior to use. Sodium (99.9%) was purchased from Sigma Aldrich and used as received. The UV-vis absorption spectra were recorded on a Shimadzu 2600i UV-visible Spectrophotometer. The ¹H NMR spectra were measured using Bruker Ascend-500 spectrometer (500 MHz for ¹H) and referenced to the resonances of the corresponding solvent used. The low-temperature NMR experiment was controlled by a Cryo Diffusion cryogenic tank probe, and liquid N₂ was used as a cooling source. The air- and moisture sensitivity of crystals Na₂-TIPS-PPP²⁻ (**2**), along with the presence of weakly coordinated THF molecules, prevented obtaining elemental analysis data.

Preparation of [{Na⁺(THF)₃]₂(TIPS-PPP²⁻)] (**2**)

THF (1.2 mL) was added to a custom-built glass system containing **1** (3.0 mg, 0.003 mmol) and excess Na metal (1.0 mg, 0.04 mmol). The mixture was allowed to stir under argon at 25 °C for 24 hours in a closed system. The initial color of the suspension was turquoise (neutral ligand), and it changed to light brown after 5 minutes and deepened to dark brown after 15 minutes. The suspension was filtered, and the dark brown filtrate was layered with 1.8 mL of hexanes. The ampule was sealed and placed at 25 °C with a slight temperature gradient. Black needles were present in solution after 14 days. Yield: 1.0 mg, 30%. ¹H NMR (THF-*d*₈, ppm, -80°C): δ = 4.84–4.89 (2H, **1**²⁻), 3.88–3.92 (2H, **1**²⁻), 3.76–3.80 (2H, **1**²⁻), 3.68–3.75 (6H, **1**²⁻), 3.12–3.16 (2H, **1**²⁻), UV-Vis (THF): λ_{max} 312, 434, 540 nm.

II. UV-Vis Spectroscopic Investigation

Sample preparation: THF (3 mL) was added to a glass ampule (O.D. 12 mm) containing **1** (0.2 mg, 0.003 mmol) and excess Na (1.0 mg, 0.04 mmol). The ampule was sealed under argon, and UV-Vis absorption spectra were monitored at different reaction times (total 24 hours) at 25 °C.

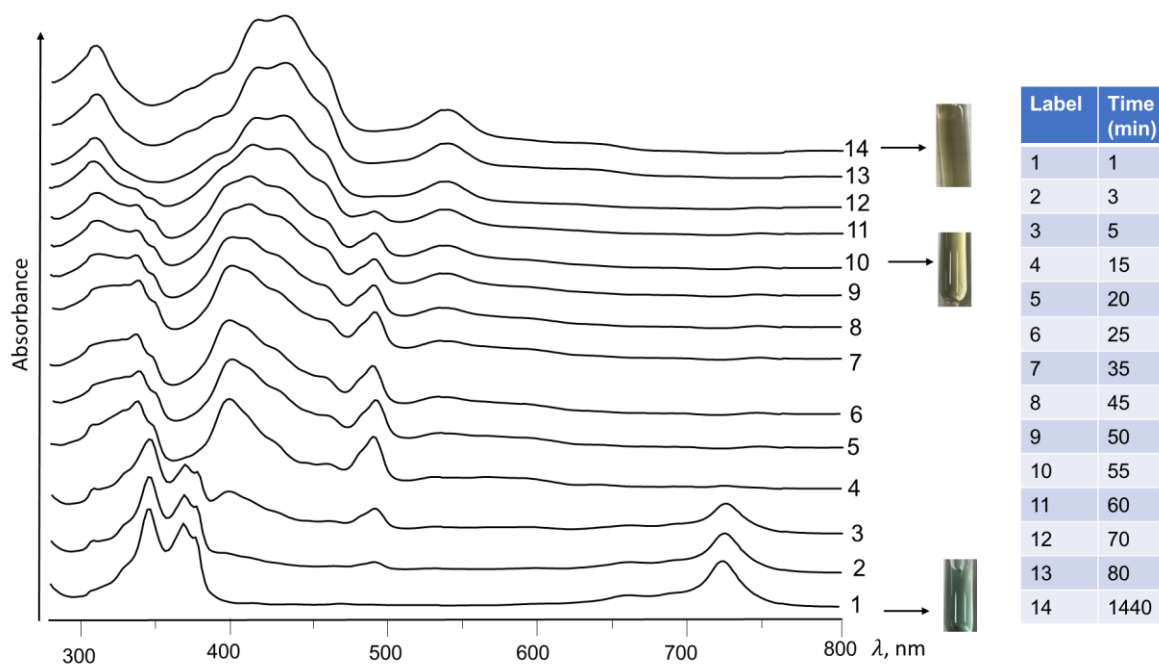


Figure S1. UV-Vis spectra of Na/**1** in THF.

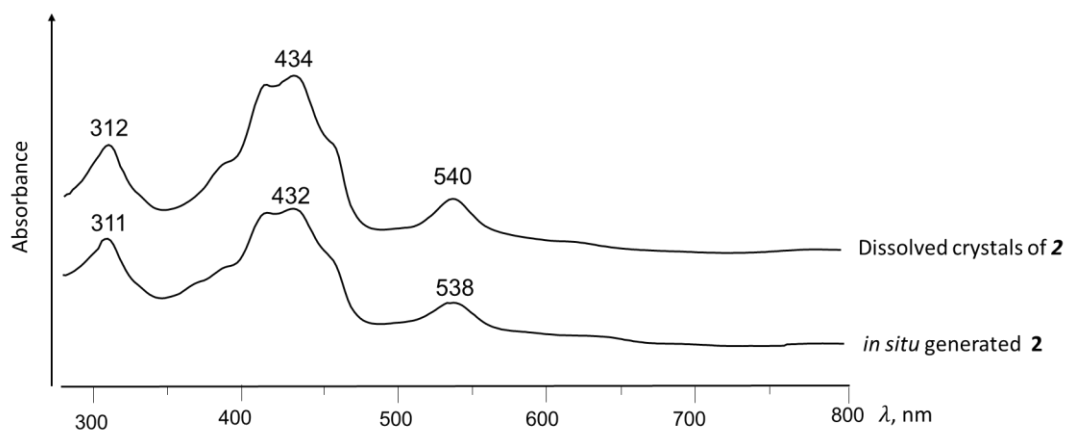


Figure S2. UV-Vis spectra of crystals of **2** dissolved and *in situ* generated **2** in THF.

III. NMR Spectroscopic Investigation

Sample preparation: **1** (2.0 mg) was dissolved in THF-*d*₈ (0.7 mL) in an NMR ampule that was sealed under argon.

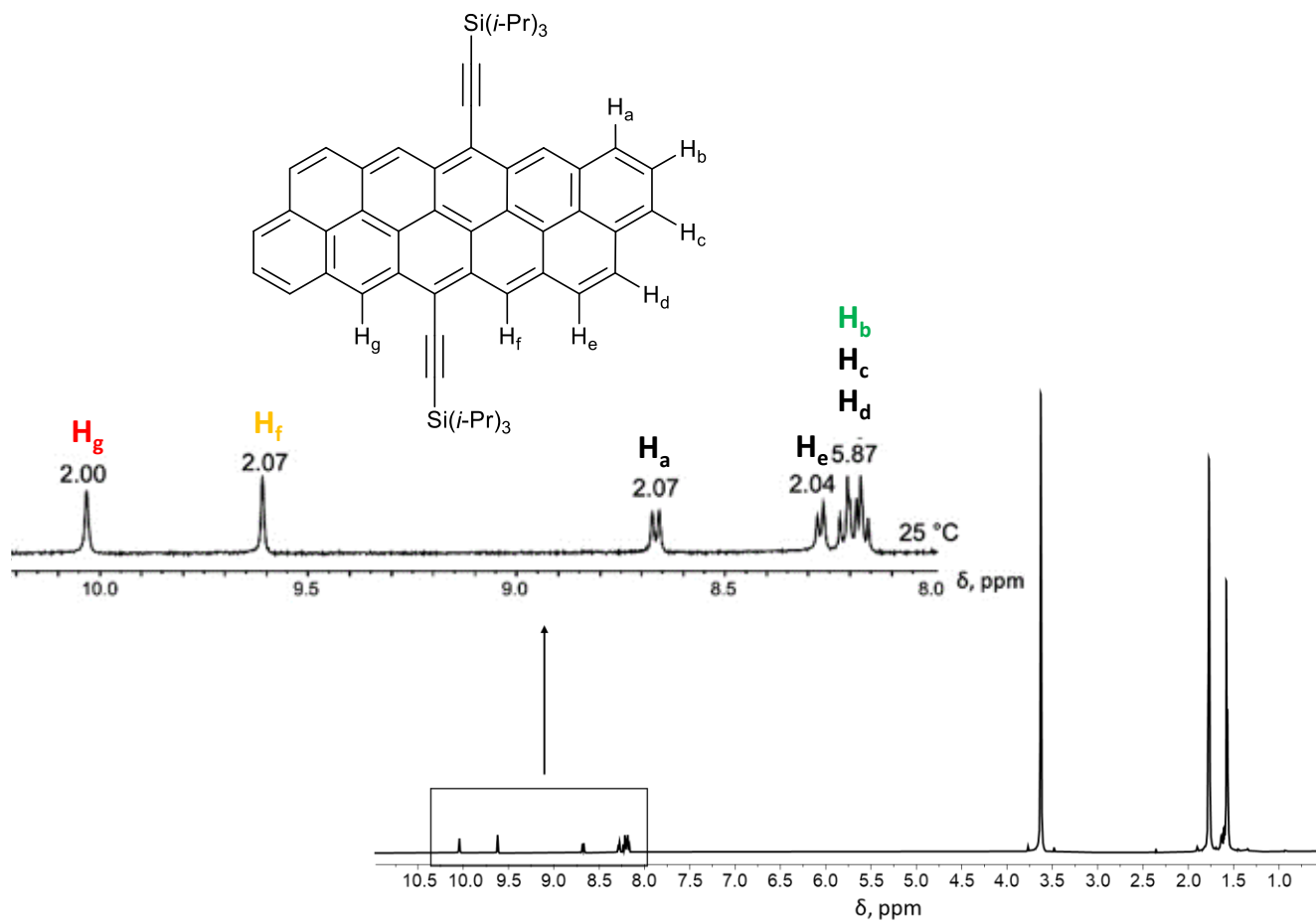


Figure S3. ¹H NMR spectrum of **1** in THF-*d*₈ at 25 °C with integrations and peak assignment.

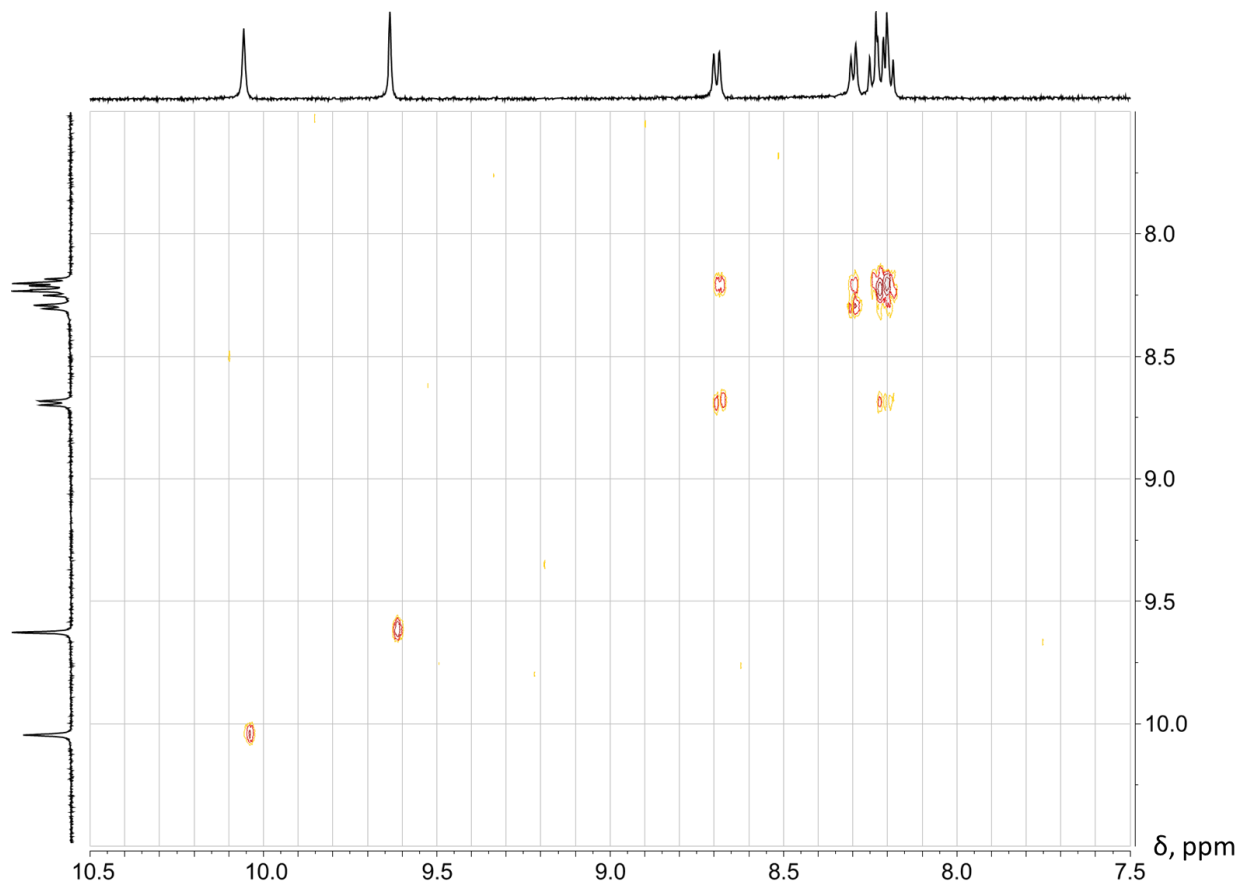


Figure S4. ^1H - ^1H COSY NMR of **1** in $\text{THF-}d_8$ at $25\text{ }^\circ\text{C}$, aromatic region.

Sample preparation: Crystals of **2** (2.0 mg) were washed several times with hexanes and dried *in vacuo*. Crystals were dissolved in THF- d_8 (0.7 mL) in an NMR ampule that was sealed under argon.

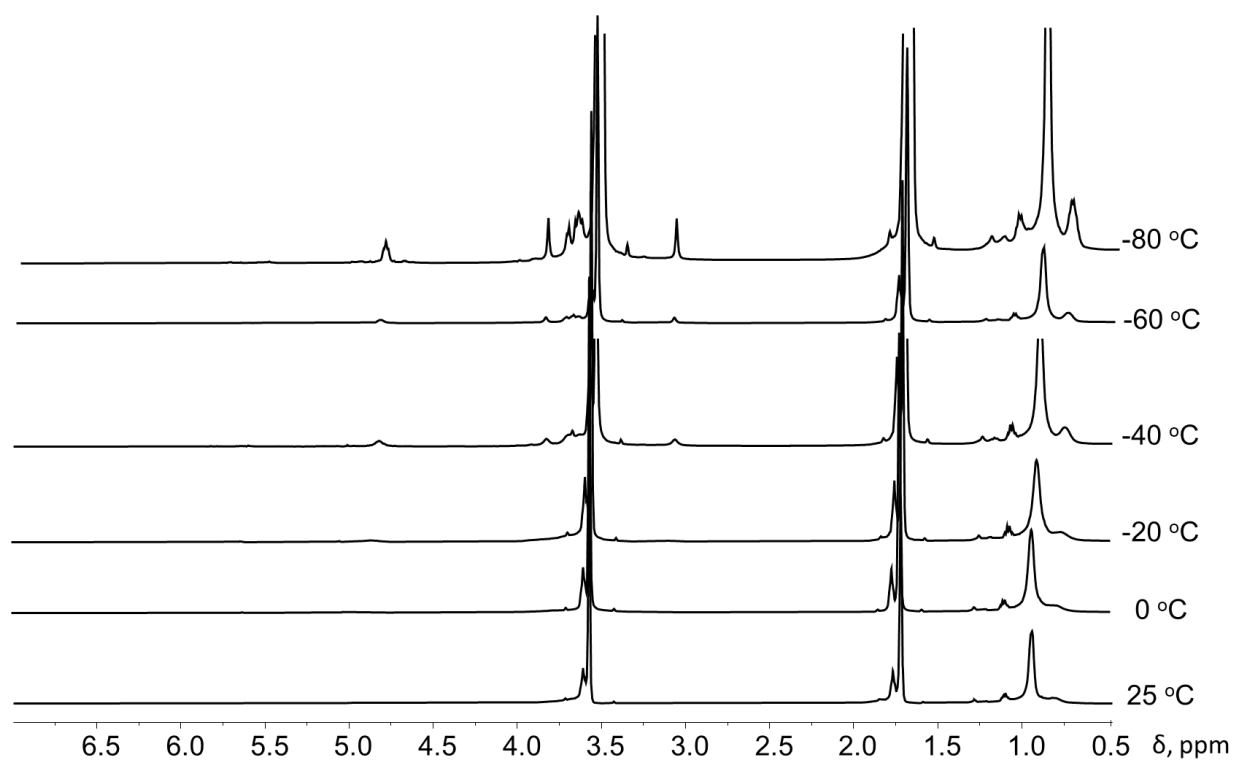


Figure S5. Variable temperature ^1H NMR spectra of **2** in THF- d_8 .

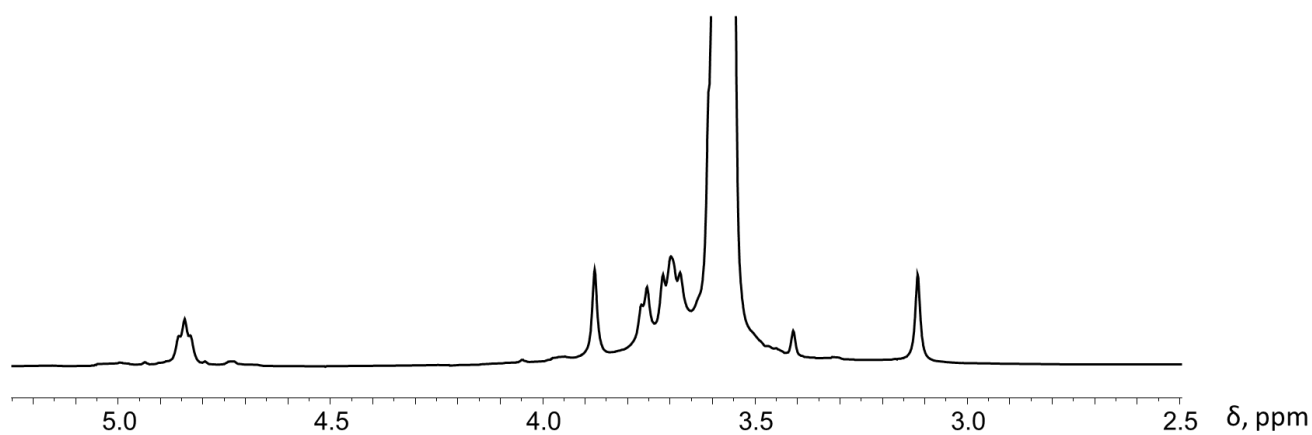


Figure S6. Zoomed in ^1H NMR spectrum of **2** in THF- d_8 at -80 °C.

IV. Crystal Structure Solution and Refinement

Data collection of **Na₂-TIPS-PPP²⁻** (**2**) was performed at 100(2) K on a Huber Kappa 4-circle system with a DECTRIS PILATUS3 X 2M(CdTe) pixel array detector using ϕ scans (synchrotron radiation at $\lambda = 0.41328 \text{ \AA}$) located at the Advanced Photon Source, Argonne National Laboratory (NSF's ChemMatCARS, Sector 15, Beamline 15-ID-D). The dataset's reduction and integration were performed with the Bruker software package SAINT (version 8.38A).^[3] Data were corrected for absorption effects using the empirical methods as implemented in SADABS (version 2016/2).^[4] The structure was solved by SHELXT (version 2018/2)^[5] and refined by full-matrix least-squares procedures using the Bruker SHELXTL (version 2019/2)^[6] software package through the OLEX2 graphical interface.^[7] All non-hydrogen atoms, including those in disordered parts, were refined anisotropically. Hydrogen atoms were included in idealized positions for structure factor calculations with $U_{\text{iso}}(\text{H}) = 1.2 U_{\text{eq}}(\text{C})$ and $U_{\text{iso}}(\text{H}) = 1.5 U_{\text{eq}}(\text{C})$ for methyl groups. In the structure model of **2**, one isopropyl group was found to be disordered. The disordered group was modeled with two orientations with their relative occupancies refined. The anisotropic displacement parameters of the disordered molecules in the direction of the bonds were restrained to be equal with a standard uncertainty of 0.004 \AA^2 . They were also restrained to have the same U_{ij} components, with a standard uncertainty of 0.01 \AA^2 . Further crystal and data collection details are listed in Table S1.

Table S1. Crystal data and structure refinement parameters for **2**.

Compound	2
Empirical formula	C ₈₀ H ₁₀₄ Na ₂ O ₆ Si ₂
Formula weight	1263.79
Temperature (K)	100(2)
Wavelength (Å)	0.41328
Crystal system	Triclinic
Space group	<i>P</i> -1
<i>a</i> (Å)	7.7756(2)
<i>b</i> (Å)	14.1848(4)
<i>c</i> (Å)	16.3912(5)
α (°)	97.3160(10)
β (°)	100.1920(10)
γ (°)	100.4480(10)
<i>V</i> (Å ³)	1725.94(8)
<i>Z</i>	1
ρ_{calcd} (g·cm ⁻³)	1.216
μ (mm ⁻¹)	0.042
<i>F</i> (000)	682
Crystal size (mm)	0.08×0.09×0.13
θ range for data collection (°)	1.041-22.173
Reflections collected	115112
Independent reflections	20479
	[<i>R</i> _{int} = 0.0430]
Transmission factors (min/max)	0.5886/0.7447
Data/restraints/params.	20479/102/436
<i>R</i> 1, ^a <i>wR</i> 2 ^b (<i>I</i> > 2σ(<i>I</i>))	0.0433, 0.1318
<i>R</i> 1, ^a <i>wR</i> 2 ^b (all data)	0.0567, 0.1399
Quality-of-fit ^c	1.094

$$R_{\text{int}} = \frac{\sum |F_o^2 - \langle F_o^2 \rangle|}{\sum F_o^2}$$

$$^a R1 = \frac{\sum ||F_o| - |F_c||}{\sum |F_o|}, \quad ^b wR2 = \frac{[\sum [w(F_o^2 - F_c^2)^2]]}{[\sum [w(F_o^2)^2]]}$$

$$^c \text{Quality-of-fit} = \frac{[\sum [w(F_o^2 - F_c^2)^2]]}{(N_{\text{obs}} - N_{\text{params}})]^{1/2}}, \text{ based on all data.}$$

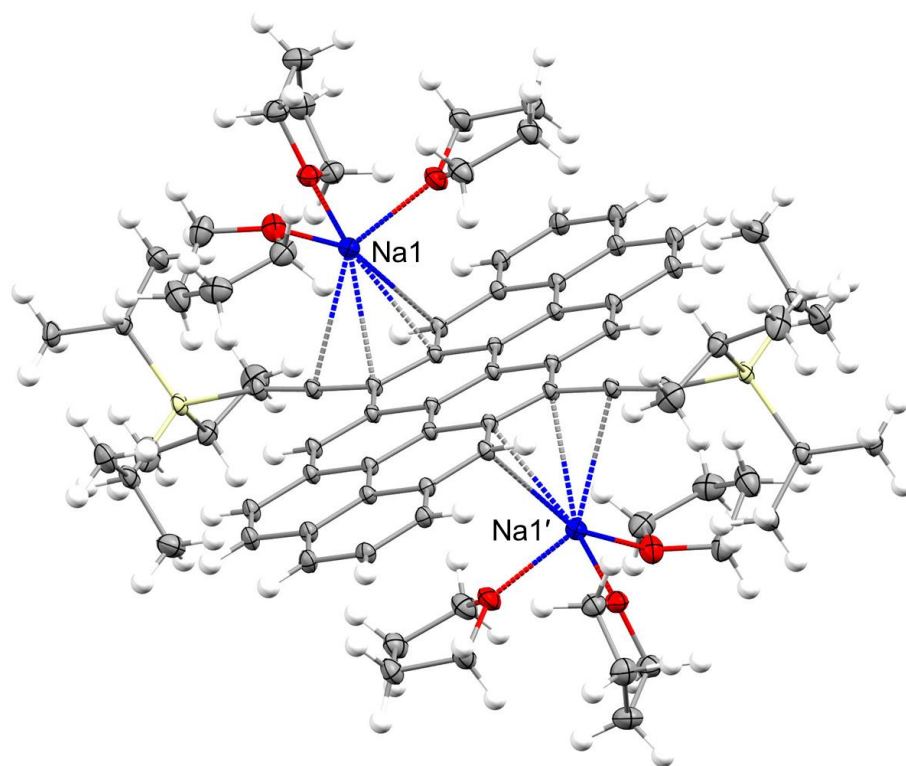


Figure S7. ORTEP diagram of the asymmetric unit of **2** with thermal ellipsoids at 50% probability level. The color scheme used: C grey, H white, O red, Na blue, Si yellow.

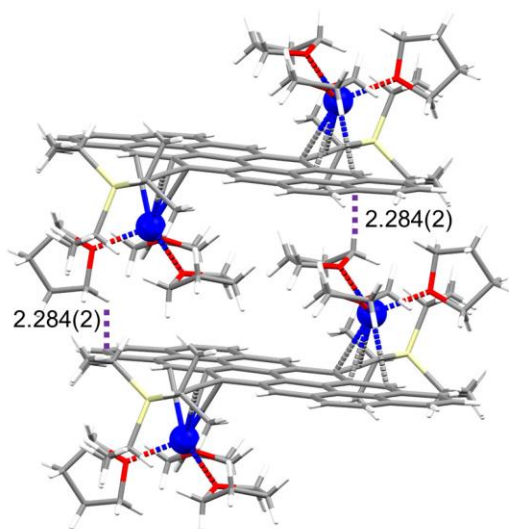


Figure S8. C–H... π interactions (\AA) in **2**.

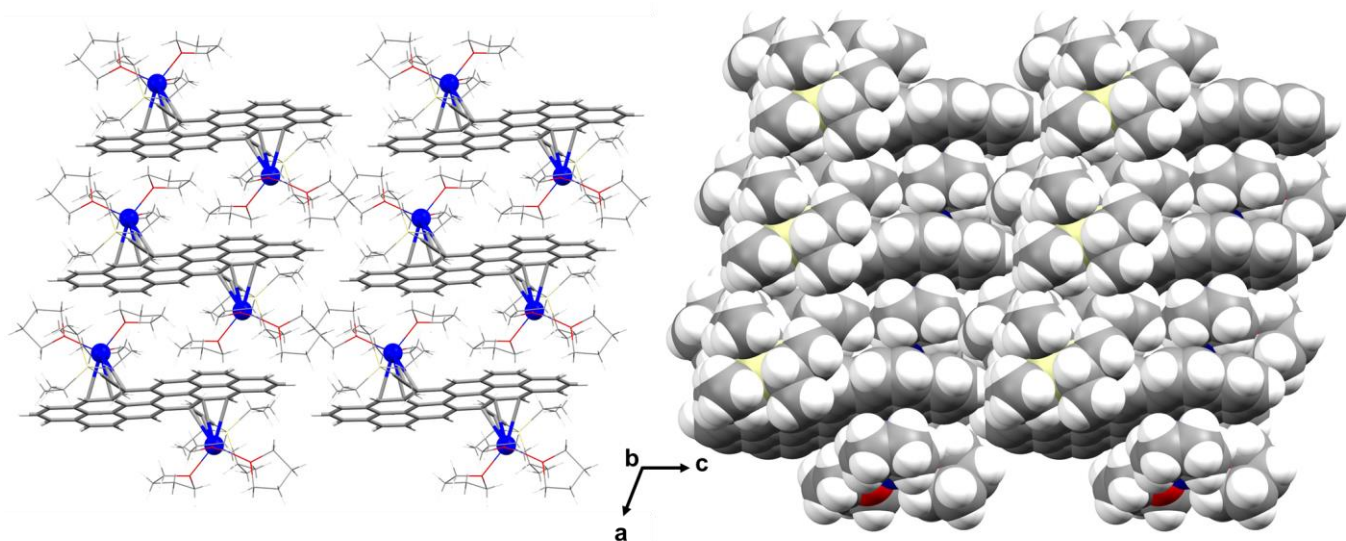
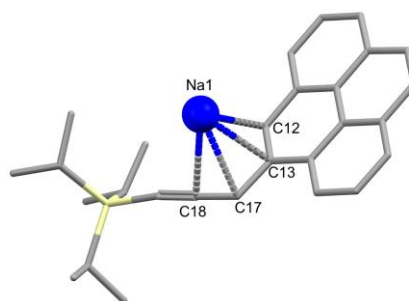
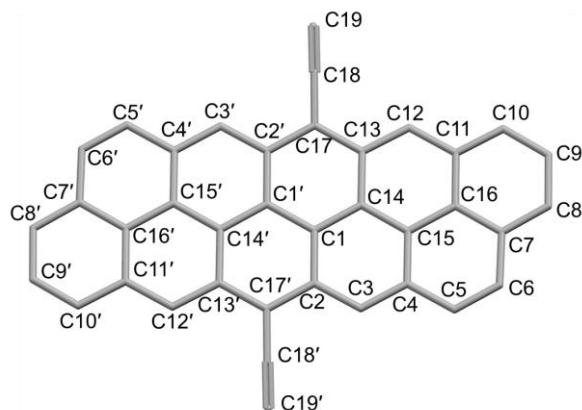


Figure S9. Solid-state packing in **2**, (left) mixed and (right) space-filling model.

Table S2. Na–C distances (Å) in **2**, along with a labeling scheme.



Bond	Distance
Na1–C12	2.7501(7)
Na1–C13	2.6342(7)
Na1–C17	2.7100(6)
Na1–C18	2.8254(6)

Table S3. X-ray and calculated (B3LYP/6-311G(d,p)) C–C bond length distances (Å) in **2**.

Bond	Distance ^a / ^b	Bond	Distance ^a / ^b
C1–C1'	1.4343(10) / 1.443	C8–C9	1.3825(9) / 1.393
C1–C2	1.4242(7) / 1.436	C9–C10	1.3859(8) / 1.391
C1–C14	1.4104(7) / 1.421	C10–C11	1.4016(8) / 1.417
C2–C3	1.3958(8) / 1.403	C11–C12	1.4125(8) / 1.411
C2–C17	1.4280(8) / 1.442	C11–C16	1.4228(7) / 1.435
C3–C4	1.3886(8) / 1.394	C12–C13	1.3912(8) / 1.396
C4–C5	1.4265(8) / 1.433	C13–C14	1.4425(7) / 1.451
C4–C15	1.4176(7) / 1.430	C13–C17	1.4272(7) / 1.438
C5–C6	1.3528(9) / 1.362	C14–C15	1.4160(7) / 1.427
C6–C7	1.4300(8) / 1.434	C15–C16	1.4182(8) / 1.426
C7–C8	1.4005(8) / 1.411	C17–C18	1.4039(7) / 1.397
C7–C16	1.4139(8) / 1.427	C18–C19	1.2217(8) / 1.231

a) X-ray bond lengths; b) Calculated bond lengths

Note: The bond length comparison of the neutral form reported in *Angew. Chem. Int. Ed.*, 2022, **61**, e202112794.

V. Computational Details

The theoretical calculations were mainly performed using the computer facilities at the Research Institute for Information Technology, Kyushu University, Japan. Molecular orbital calculations were performed using the program Gaussian 16.^[8] The geometries were optimized at the B3LYP/6-311G(d,p) level, and the optimized structures are used for the further calculations unless otherwise noted. The presence of energy minima for the geometry optimization was confirmed by the absence of imaginary modes (no imaginary frequencies). To numerically achieve accurate values, we have used a fine grid. The triisopropylsilyl (TIPS) groups were substituted with trimethylsilyl (TMS) groups. NICS values were estimated using the GIAO-B3LYP/6-311+G(d,p) methods. The NICS(1.7) π zz values at a height of 1.7 Å above the molecular plane employing σ -only model were used to obtain the effect of the π contribution only.^[9] The hydrogen atoms for the σ -only model and ghost atoms were generated by using Aroma software.^[10] The NICS values calculated for the optimized geometries and crystal structure are found to be similar (Table S4).

Table S4. NICS(1.7) π zz values.

Ring	TIPS-PPP crystal	TMS-PPP optimized	TIPS-PPP ²⁻ crystal	TMS-PPP ²⁻ optimized
A	-19.6	-20.6	-6.1	-6.9
B	-21.8	-23.5	0.7	-0.7
C	-17.0	-18.7	3.9	4.7
D	-12.5	-15.3	-9.2	-9.9
E	-5.3	-7.6	-8.3	-9.3

The current density plotted onto the ACID were generated using the programs Gaussian 16 and AICD 3.0.^[11] The ring current analysis was performed with the CSGT method at the B3LYP/6-311+G(d,p) level with IOp(10/93=2). The magnetic field was applied parallel to z-axis (0 0 1). The number of points of cartesian grid was set as 160000.

The molecular electrostatic potential (MEP) maps were calculated at the B3LYP/6-311G(d,p) level.

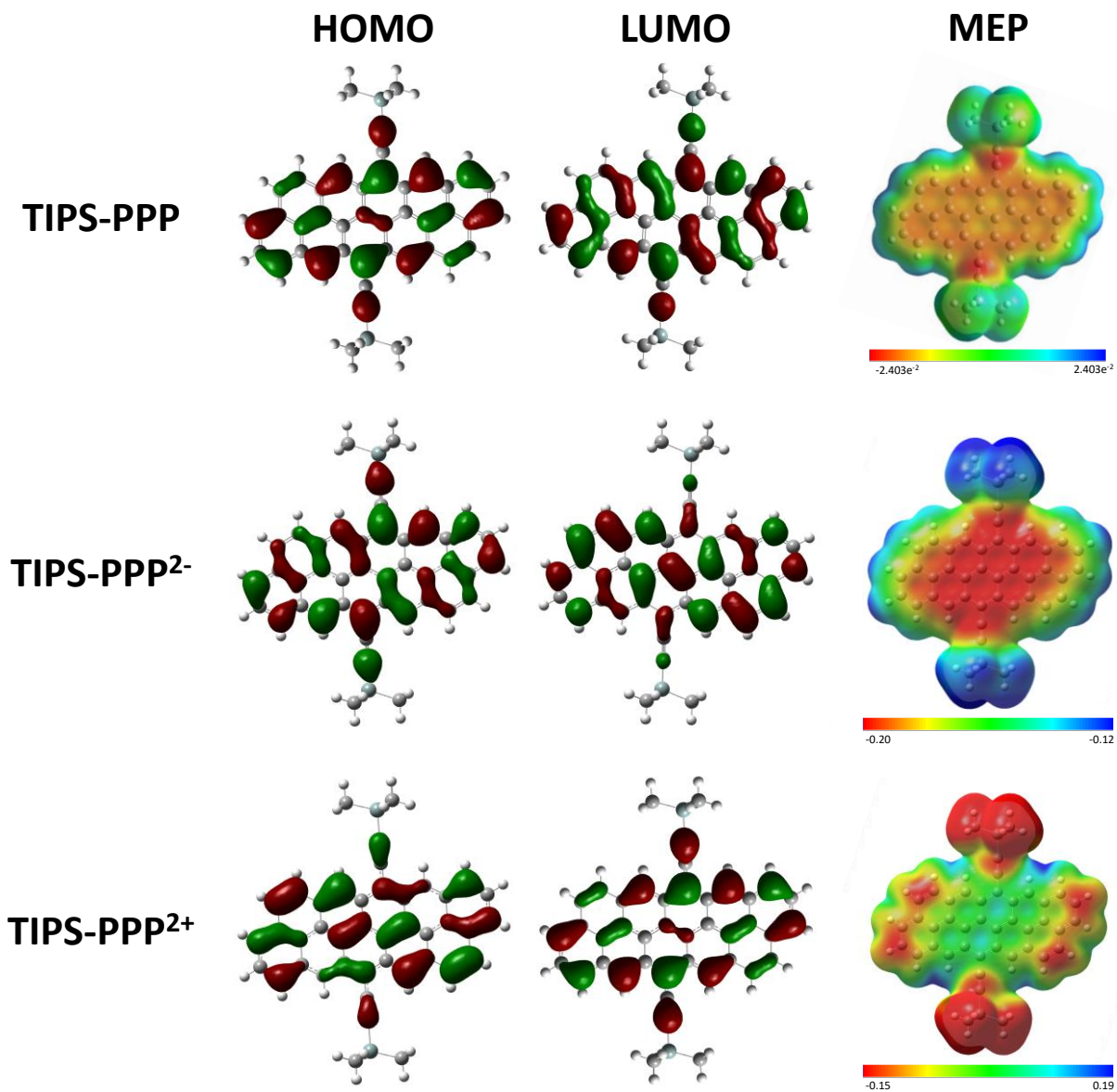


Figure S10. HOMO and LUMO of TIPS-PPP, TIPS-PPP²⁻, and TIPS-PPP²⁺ and their calculated molecular electrostatic potential maps.

VI. References

- [1] N. V. Kozhemyakina, J. Nuss and M. Jansen, *Z. Für Anorg. Allg. Chem.*, 2009, **635**, 1355–1361.
- [2] T. Jousselein-Oba, M. Mamada, K. Wright, J. Marrot, C. Adachi, A. Yassar and M. Frigoli, *Angew. Chem. Int. Ed.*, 2022, **61**, e202112794.
- [3] SAINT; part of Bruker APEX3 software package (version 2017.3-0); Bruker AXS, 2017.
- [4] SADABS; part of Bruker APEX3 software package (version 2017.3-0); Bruker AXS, 2017.
- [5] G. M. Sheldrick, *Acta Crystallogr.*, 2015, **A71**, 3-8.
- [6] G. M. Sheldrick, *Acta Crystallogr.*, 2015, **C71**, 3-8.
- [7] O. V. Dolomanov, L. J. Bourhis, R. J. Gildea, J. A. K. Howard and H. Puschmann, *J. Appl. Crystallogr.*, 2009, **42**, 339-341.
- [8] Gaussian 16, Revision A.03, M. J. Frisch, G. W. Trucks, H. B. Schlegel, G. E. Scuseria, M. A. Robb, J. R. Cheeseman, G. Scalmani, V. Barone, G. A. Petersson, H. Nakatsuji, X. Li, M. Caricato, A. V. Marenich, J. Bloino, B. G. Janesko, R. Gomperts, B. Mennucci, H. P. Hratchian, J. V. Ortiz, A. F. Izmaylov, J. L. Sonnenberg, D. Williams-Young, F. Ding, F. Lipparini, F. Egidi, J. Goings, B. Peng, A. Petrone, T. Henderson, D. Ranasinghe, V. G. Zakrzewski, J. Gao, N. Rega, G. Zheng, W. Liang, M. Hada, M. Ehara, K. Toyota, R. Fukuda, J. Hasegawa, M. Ishida, T. Nakajima, Y. Honda, O. Kitao, H. Nakai, T. Vreven, K. Throssell, J. A. Montgomery, Jr., J. E. Peralta, F. Ogliaro, M. J. Bearpark, J. J. Heyd, E. N. Brothers, K. N. Kudin, V. N. Staroverov, T. A. Keith, R. Kobayashi, J. Normand, K. Raghavachari, A. P. Rendell, J. C. Burant, S. S. Iyengar, J. Tomasi, M. Cossi, J. M. Millam, M. Klene, C. Adamo, R. Cammi, J. W. Ochterski, R. L. Martin, K. Morokuma, O. Farkas, J. B. Foresman, and D. J. Fox, Gaussian, Inc., Wallingford CT, 2016.
- [9] (a) A. Stanger, *J. Org. Chem.*, 2006, **71**, 883-893; (b) A. Stanger, *J. Org. Chem.*, 2010, **75**, 2281-2288; (c) R. Gershoni-Poranne and A. Stanger, *Chem. Eur. J.*, 2014, **20**, 5673-5688.
- [10] Z. Wang, *ChemRxiv*, 2024, DOI: 10.26434/chemrxiv-2024-mjmmj8.
- [11] (a) R. Herges and D. Geuenich, *J. Phys. Chem. A*, 2001, **105**, 3214-3220; (b) D. Geuenich, K. Hess, F. Köhler and R. Herges, *Chem. Rev.*, 2005, **105**, 3758-3772.